Article

Can the Flap of a Butterfly's Wings Shift a Tornado into Texas—Without Chaos?

Yoshitaka Saiki [1,*] and James A. Yorke [2,3,4]

1 Graduate School of Business Administration, Hitotsubashi University, Tokyo 186-8601, Japan
2 Institute for Physical Science and Technology, University of Maryland, College Park, MD 20742, USA; yorke@umd.edu
3 Department of Mathematics, University of Maryland, College Park, MD 20742, USA
4 Department of Physics, University of Maryland, College Park, MD 20742, USA
* Correspondence: yoshi.saiki@r.hit-u.ac.jp

Abstract: In our title, "chaos" means there is a positive Lyapunov exponent that causes the tornado to move. We are asserting that a positive Lyapunov exponent is not always needed to have a butterfly effect. Lorenz's butterfly effect initially appeared in meteorology and has captured the imaginations of people for applications to all kinds of fields. We feel it is important to understand simpler non-meteorological models to understand the additional aspects of the butterfly effect. This paper presents simple linear map models that lack "chaos" but exhibit a butterfly effect: our simplest model does not have any positive Lyapunov exponents but still exhibits a butterfly effect, that is, temporary exponential growth from a tiny perturbation such as one infected mosquito setting off an epidemic outbreak. We focus on a 24-dimensional version of the map where a significant butterfly effect is observed even though the only Lyapunov exponent is 0. We introduce a linear "infected mosquito" model that shows how off-diagonal matrix entries can cause a finite-time growth rate. We argue that the degree of instability in our systems can be better measured by its finite-time growth rate. Our findings suggest that even in linear systems, off-diagonal matrix entries can significantly impact the system's behavior and be more important than the Lyapunov exponents in higher-dimensional systems. A focus on finite-time growth rates can yield valuable insights into the system's dynamics.

Keywords: butterfly effect; sensitive dependence on initial conditions; instability; Zika toy model

1. Introduction

The butterfly effect described by Edward Lorenz [1,2] has become a central concept in the study of nonlinear systems. This effect is typically associated with "chaos" and characterized by positive Lyapunov exponents. Of course, the Lyapunov exponents of a trajectory are a partial description of what happens near the trajectory based on a linearization of the dynamics near the trajectory. That analysis is greatly simplified if the system is linear since the linearization of all trajectories is the same. By studying linear systems, we gain clarity about the relationship between Lyapunov exponents and the butterfly effect, which can be quantified by what we call the "butterfly number" in Section 2. By presenting a butterfly effect in simple linear systems, we hope to contribute to a deeper understanding of the role of dimensionality and off-diagonal terms in the linearization of the dynamics of physical systems. We are not creating a new butterfly effect here, but we are simply pointing out how it can occur in systems for which there is no positive exponent, and we use only elementary mathematical techniques.

Sensitive dependence on initial conditions. There are several ways of characterizing sensitive dependence on initial conditions [3–5]. Sensitive dependence on initial conditions is defined by J. Guckenheimer [5] in any dimension as follows: there exists a positive ε such that, for all x in the phase space and all $\delta > 0$, there is some y that is within a distance δ of x and there is some n such that $d(T^n x, T^n y) > \varepsilon$. The phrase "sensitive dependence on initial

conditions" was used by D. Ruelle [6] to indicate some exponential rate of divergence of the orbits of nearby points, which has often been used to characterize chaos in the literature. Guckenheimer's definition does not require there to be a positive Lyapunov exponent, but it is challenging to find a natural system that satisfies their definition but has no trajectories with a positive Lyapunov exponent.

The ancient history of sensitivity to initial conditions. The following seems to describe how a tiny perturbation can lead to large changes through a pattern of increasingly big effects over a finite amount of time. Benjamin Franklin included a version of the tale about horseshoes and battles in their Poor Richard's Almanack. Franklin's was far from the first version. (Benjamin Franklin, Poor Richards Almanack, June 1758, The Complete Poor Richard Almanacks, facsimile ed., vol. 2, pp. 375–377) [7].

The horseshoe nail cascade effect: "For Want of a Nail", an example of "finite-time sensitive dependence"

For want of a nail the shoe was lost;
For want of a shoe the horse was lost;
For want of a horse the rider was lost;
For want of a rider the message was lost;
For want of a message the battle was lost;
For want of a battle the kingdom was lost;
Furthermore, all for the want of a horseshoe nail.

We believe that scientists and mathematicians were among the last people to learn about sensitivity to initial conditions. The above nail tale has been discussed by other authors, including Lorenz [8] and Shen [9]. We mention it here to contrast it with our "parable about angles" in Section 3.

Dynamics of the Lorenz's 1969 paper [2]. The Lorenz paper from 1969 analyzed a high dimensional spatial multi-scale model, describing how energy at the model's smallest scales could propagate quickly to the largest scales, provided there was lots of energy in the smallest scales. Perhaps huge numbers of energetic butterflies could provide that energy, although the article did not mention butterflies. Wikipedia's "butterfly effect" [10] says: "According to Lorenz, when he failed to provide a title for a talk he was to present at the 139th meeting of the American Association for the Advancement of Science in 1972, Philip Merilees concocted 'Does the flap of a butterfly's wings in Brazil set off a tornado in Texas?' as a title." A single flapping of a butterfly causes chaos in the Lorenz paper from 1963 [1], whereas the butterfly effect in the Lorenz paper from 1969 [2] is caused by the propagation of huge numbers of flapping butterflies. The analysis of the Lorenz's 1969 model's linearly unstable solutions was first documented in Shen et al. [11].

Outline of the paper. In Section 2, we begin with a mosquito model instead of a butterfly. We introduce a simple linear one-space-dimension map. We show that the map shows a butterfly effect, "the sensitive dependence on initial conditions" for some finite times, although the map is not chaotic in the sense that it does not have positive Lyapunov exponents. In Section 3, we describe another well-known multi-dimensional torus map where the coordinates are angles. We investigate the numerics of the map in Section 4. In Section 5, we explain the known mathematical results and introduce a conjecture together with some numerical evidence. We discuss the related works and summarize our results in Section 6.

2. Linear *K*-Dimensional System Showing the Butterfly Effect

Models for the spread of Zika-infected mosquitoes. Jeffery Demers et al. [12] investigated a heterogeneous, two-space-dimensional model of infected Aedes mosquitoes. Some species of mosquitoes, such as Aedes, can become infected and can transmit diseases such as Zika, and they have little mobility during their lifetimes. This means it can be effective to focus the killing of mosquitoes in the small areas where the disease exists. See our discussion section (Section 6.2) for New York Times articles that discuss the Zika outbreak in Miami, Florida, and elsewhere. The World Health Organization recently de-

clared mosquito-borne Zika an "international public health emergency". Our focus is on how a new exponentially growing outbreak is local early in the outbreak. Hence, a new outbreak can sometimes be interrupted using only local strategies for killing mosquitoes, as opposed to expensive strategies that would try to (temporarily) eradicate mosquitoes in a large region. Of course, "exponential growth" is temporary. Our model is spatially one-dimensional, but it is easy to convert it into a two-space dimension model, provided the winds generally blow mosquitoes in one direction.

A one-space-dimensional infected-mosquito model. We assume that there is a line of land tracts numbered $k = 1, 2, 3, \ldots$, perhaps along a road. We imagine that these regions all have a similar area, perhaps one square hectare. Our model's infected mosquitoes live for one time period, and in one time period, each infected mosquito in tract k has $a_k + b_k$ progeny, which we imagine is approximately 2. We assume $a_k \approx 1$ mosquitoes stay in tract k and $b_k \approx 1$ are blown by a constant wind into tract $k + 1$. Writing x_k for the number of infected mosquitoes in tract k yields the following dynamical model, which we call our "(infected-) mosquito model".

$$(x_1, x_2, \ldots, x_K) \mapsto (a_1 x_1, a_2 x_2 + b_1 x_1, \ldots, a_K x_K + b_{K-1} x_{K-1}), \tag{1}$$

This equation can be viewed as a linearization about $y_j = 0$ for all coordinates j—of a spatial logistic-based map. One possibility uses $g(y) := y(1 - y)$ where $y = y_k$ is a density at each tract k with a maximum sustainable value of 1. The nonlinear equation is the following:

$$(y_1, y_2, \ldots, y_K) \mapsto \big(g(a_1 y_1), g(a_2 y_2 + b_1 y_1), \ldots, g(a_K y_K + b_{K-1} y_{K-1})\big). \tag{2}$$

Recall that y_k is a density while x_k is the number of mosquitoes. Huge values of x_k correspond to moderate values of y_k.

We can write (1) in vector format, writing $X = (x_1, x_2, \ldots, x_K)$. For time $n \geq 0$, let $X^n = (x_1^n, x_2^n, \ldots, x_K^n)$ be a trajectory of (1) determined by

$$X^{n+1} = M_{gen} X^n, \tag{3}$$

where we define M_{gen} as follows:

$$M_{gen} = \begin{pmatrix} a_1 & 0 & 0 & 0 & 0 & 0 & \cdots & 0 \\ b_1 & a_2 & 0 & 0 & 0 & 0 & \cdots & 0 \\ 0 & b_2 & a_3 & 0 & 0 & 0 & \cdots & 0 \\ 0 & 0 & b_3 & a_4 & 0 & 0 & \cdots & 0 \\ 0 & 0 & 0 & b_4 & a_5 & 0 & \cdots & 0 \\ 0 & 0 & 0 & 0 & b_5 & a_6 & \cdots & 0 \\ & & & \vdots & & & & \\ 0 & 0 & 0 & & \cdots & & b_{K-1} & a_K \end{pmatrix}. \tag{4}$$

There can be rapid growth over time for large K when $a_k + b_k > 1$ for all k. We invite the reader to try various choices of coefficients. This model gives many cases to consider.

Notation for "spatially homogeneous" matrices. Tri-diagonal matrix. In this part, we comment on the case where a map is determined by the tri-diagonal matrix M_{abc}. Assume that the $K \times K$ matrix M_{abc} is a tri-diagonal matrix with the following form:

$$M_{abc} = \begin{pmatrix} a & b & 0 & 0 & & 0 & 0 & \cdots & 0 \\ c & a & b & 0 & & 0 & 0 & \cdots & 0 \\ 0 & c & a & b & & 0 & 0 & \cdots & 0 \\ 0 & 0 & c & a & & b & 0 & \cdots & 0 \\ 0 & 0 & 0 & c & & a & b & \cdots & 0 \\ 0 & 0 & 0 & 0 & & c & a & \cdots & 0 \\ & & & \vdots & & & & & \\ 0 & 0 & 0 & & & \cdots & & c & a \end{pmatrix}, \tag{5}$$

where a, b, and c are non-negative real numbers. This type of matrix is considered to commonly appear in a linearized system in various nonlinear phenomena. An example with a linearization that is somewhat similar is the Gledzer–Okhitani–Yamada (GOY) shell model of fluid turbulence that mimics the Galerkin spectral equations of the Navier–Stokes equations (A detailed analysis of this matter will be reported elsewhere as a joint work with Miki U. Kobayashi.). It is a system of N-dimensional complex-valued ordinary differential equations with the following form [13]:

$$\left(\frac{d}{dt} + \nu k_n^2 \right) u_n = i[c_n^{(1)} u_{n+1}^* u_{n+2}^* + c_n^{(2)} u_{n-1}^* u_{n+1}^* + c_n^{(3)} u_{n-1}^* u_{n-2}^*] + f\delta_{n,1},$$

where f is a forcing parameter, $\delta_{n,1}$ is a Kronecker delta, and $c_1^{(2)} = c_1^{(3)} = c_2^{(3)} = c_{N-1}^{(1)} = c_N^{(1)} = c_N^{(2)} = 0$, and $c_n^{(1)} = k_n, c_n^{(2)} = -k_{n-2}, c_n^{(3)} = -k_{n-3}$ with $k_n = 2^{n-4}$ for other n.

The eigenvalues the matrix M_{abc} are

$$\lambda_k = a + 2\sqrt{bc} \, \cos\left[\frac{k\pi}{K+1} \right], \quad k = 1, \ldots, K; \tag{6}$$

the **Lyapunov number** is $\max_k |\lambda_k|$, and the Lyapunov exponent is the log of the Lyapunov number. From this formula, we obtain an inequality:

$$\lambda_k \leq a + 2\sqrt{bc}, \quad k = 1, \ldots, K. \tag{7}$$

See [14] for details. For large K, $\max_k \lambda_k \simeq a + 2\sqrt{bc}$. Of course if $b = c$, the right-hand side is $a + b + c$.

Define the **butterfly number** (or **the local Lyapunov number**) of the tri-diagonal matrix to be the column sum of the typical column of the matrix,

$$\beta(M_{abc}) := a + b + c. \tag{8}$$

For positive a, b, c,

$$\beta(M_{abc}) > \max |\lambda_k|,$$

which is the largest Lyapunov number. Hence, the temporary growth rate is $\beta(M_{abc})$. If $a = b = 0$ and $c = 2$, the infected mosquitoes double each generation (until the open boundary at tract K is reached) while the Lyapunov number is 0 (and the Lyapunov exponent is $-\infty$. If $X = (\ldots, x_k, \ldots)$ has no negative entries and the first and last entries are 0, then $\sum_k x_k' = \beta(M_{abc}) \sum_k x_k$ where $x_k' = (M_{abc}X)_k$. Hence, the sum of the entries increases by a factor of $a + b + c$ from one application of M_{abc}.

To focus on a truly elementary case, we focus on the case where all $a = c = 1$ and $b = 0$ or, even more simply $a = 0, c = 1$, and $b = 0$.

Our model still has a one-space dimension and is spatially homogeneous (except at entries 1 and K).

$$(x_1, x_2, \ldots, x_K) \mapsto (x_1, x_2 + x_1, \ldots, x_K + x_{K-1}), \tag{9}$$

the one-mosquito-generation map with K land tracts. Assume that, at time 0, there is one infected mosquito, and it is in tract 1.

As we describe later, tract k at time n for $k \geq n \geq 1$ will have $\binom{k}{n}$ infected mosquitoes. Recall that $\binom{k}{n} = \frac{k!}{n!(k-n)!}$, which is 0 if $n > k$. Figure 1 displays the distribution. It seems to show a pattern analogous to the pipe flow [15], where the center of the distribution at time n is tract $\frac{n}{2}$. Of course, pipe flow is a nonlinear process, while our model emphasizes only the linear growth phase. See our remarks in Section 6 on the work of Kaneko and Crutchfield on pipe flow. Later, we discuss how the center of the infected mosquito distribution moves, as seen in Figure 1. Clearly, in reality, the population of infected mosquitoes exists against a background of a large uninfected population. The number of infected mosquitoes would eventually saturate, a fact not reflected in our model.
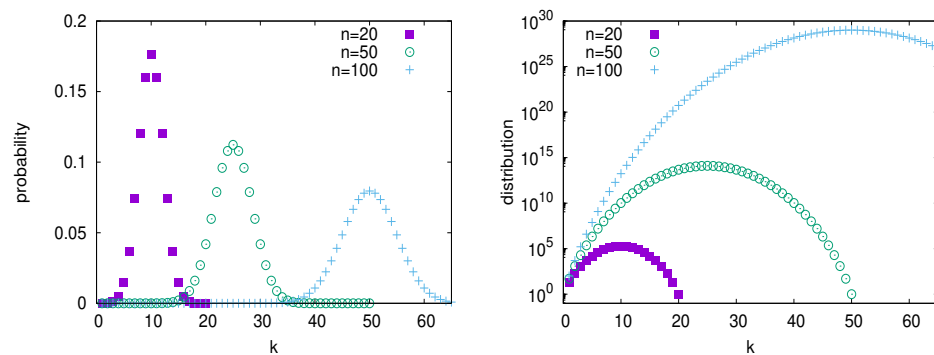

Figure 1. The mosquito model solution $\binom{n}{k}$ where k is the number of the tract (or location), and n is time. Normalized binomial probability distributions $\binom{n}{k}2^{-n}$ (**left**) and log plot of $\binom{n}{k}$ (**right**) are shown for $n = 20, 50, 100$. Both have a mean $\frac{n}{2}$ and standard deviation $\frac{\sqrt{n}}{2}$. The center of the distribution, which is the mean, moves as n changes, and the distribution on the left has sum $= 1$, and on the right, $\binom{n}{k}$ has sum $= 2^n$. See Figure 2 for the movement of the peak as time n increases.
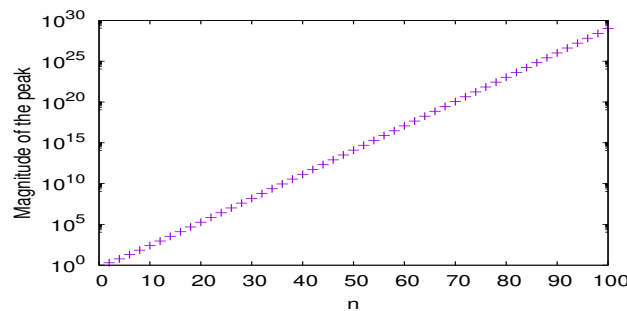

Figure 2. Peak value $\binom{n}{n/2}$ of the distribution $\binom{n}{k}$. The binomial is the vector $X^n = M^n(X)$ for the initial value $X = e_1 = (1, 0, 0, \ldots)$—with respect to n for even n, where n can be thought of as time measured in mosquito generations.

One infected Miami mosquito. We examine a finite line of K tracts where all $x_k \geq 0$, so eventually, if n is large, the largest value of X^n occurs at the end, i.e., at x_K. In Miami, the winds tend to blow from west to east, and since Miami is on the western edge of the Atlantic Ocean, its mosquitoes in the last tract can be blown into the ocean and cease to be a problem. We assume an outbreak starts with one mosquito infected with the Zika virus. Here, we aim at simplicity. A more detailed model such as Demers' would be spatially heterogeneous and two-dimensional, which would include people infecting mosquitoes and mosquitoes infecting people. The resulting behavior could be similar to the explosive growth we observe here, depending on the details, possibly growing even faster.

Again, we can write (9) in vector format, writing $X = (x_1, x_2, \ldots, x_K)$. For time $n \geq 0$, let $X^n = (x_1^n, x_2^n, \ldots, x_K^n)$ be a trajectory of (9) determined by

$$X^{n+1} = MX^n, \tag{10}$$

where M is the two-diagonal matrix $K \times K$ matrix M_{101}, i.e., $a = c = 1, b = 0$.

Let e_k denote the vector whose k^{th} entry is 1 and its other entries are 0. The finite-dimensional matrix M (with dimension K) has only one eigenvector, $e_K := (0, \ldots, 0, 1)$, and its eigenvalue is 1, so all of the map's Lyapunov exponents are 0. The multiplicity of the eigenvector is K. The matrix M is a Jordan block matrix.

The time n mosquito distribution $M^n e_1$ for Equation (10). The natural initial condition for the mosquito model is $e_1 = (1, 0, \ldots, 0)$. For this initial state e_1, i.e., one mosquito in tract 1 at time 0, the number of infected mosquitoes at any later time $n \geq 0$ on tract k where $k \leq n$, K is $\binom{n}{k}$, and the total number of infected mosquitoes is 2^n provided $n \leq K$.

The vector $M^n e_1$ at time n is the left-most column of M^n, and its last coordinate x_K is $\binom{n}{K-1}$, which, of course, is 0 for $n < K - 1$. Since K is fixed, x_K^n grows slower than exponentially as n increases.

If the last coordinate x_K is 0 at time n, then the total number of infected mosquitoes at time $n + 1$ is twice the total at time n, i.e., for time n,

$$\sum_{k=1}^{K} x_k^{n+1} = 2 \sum_{k=1}^{K} x_k^n. \tag{11}$$

In this case, generally, when time n is less than K, the mosquitoes have not yet reached the last tract, K, and the application of M doubles the sum. See Figure 1 (right). As mentioned above, there is only one eigenvector of M, and that is $(0, \ldots, 0, 1)$ i.e., all entries except the last are 0, and the last is one. This is an eigenvector with an eigenvalue of 1 with a multiplicity of K. Hence, the rapid growth of the sum of the coordinates seen in Equation (11) is not because of the eigenvalue but is **a result of the off-diagonal terms that do not contribute to the eigenvalues**. While Lyapunov exponents come from linearizations, they do not reflect all of the information in the linearization. Since our map is linear, this point is easier to see.

3. Converting Each x_k into a Direction on a Circle

Skew-product map of a torus. The special mosquito map can be converted into a well-known "skew-product map" on a torus. Each x_k becomes an angle $\theta_k = x_k$ mod 1 in a circle that we represent by $[0, 1)$, and we identify the ends, 0 and 1, by computing each θ_k, mod 1. In a physics context, angles are often referred to as phases.

It is traditional to include an irrational α, in the rotation map on the first circle $\mathbb{T}^1$,

$$\theta_1 \mapsto \theta_1 + \alpha \mod 1, \tag{12}$$

and having α irrational is required for the results in Section 5. We also obtain maps of any finite dimension, including the long-studied two-dimensional map on the two-torus $\mathbb{T}^2$ [16–19],

$$(\theta_1, \theta_2) \mapsto (\theta_1 + \alpha, \theta_2 + \theta_1) \mod 1, \tag{13}$$

where, in this paper, "v mod 1" signifies that mod 1 is always applied to each coordinate of a vector v.

We investigate the map of the K-dimensional torus $\mathbb{T}^K$ because it exhibits a butterfly effect (via the perturbation of angles):

$$(\theta_1, \theta_2, \ldots, \theta_K) \xrightarrow{F} (\theta_1 + \alpha, \theta_2 + \theta_1, \ldots, \theta_K + \theta_{K-1}) \mod 1, \tag{14}$$

where K is fairly large, perhaps $K \simeq 24$. We choose 24 for illustrations because the width of Texas is approximately 2^{24} times the size of a 3 cm. butterfly.

Each coordinate value, θ_k, is a point on a circle, so we can refer to it as a "direction" or an angle. Each perturbation of direction θ_k on iterate n perturbs the direction θ_{k+1} on iterate $n+1$ and later. We make a conjecture about the behavior of this equation in Section 5. Write $\Theta = (\theta_1, \theta_2, \ldots, \theta_K)$, and for $n \geq 0$, let Θ^n be a trajectory of (14).

Notice that the kth coordinate at time n, namely Θ_k^n, only depends on Θ_i^{n-1} for $i \leq k$, so that Θ^n is a trajectory of (14), and for $K = 2$, it is a vector of length 2, so then it is a trajectory of (13). Writing (14) in vector format

$$\Theta^{n+1} = M\Theta^n \bmod 1. \tag{15}$$

Notice that because all entries of M are integers, the map $[M^n(\Theta)] \bmod 1$ (applying $\bmod 1$ only after n applications of M) is identical to $[M(\Theta) \bmod 1]^n$, applying $\bmod 1$ at each iterate. Furthermore, if we make numerical studies in which each coordinate remains less than 1, the results are meaningful regardless of whether $\bmod 1$ is applied.

A parable about angles. This part is about angles or orientations. We now propose a parable about changing directions, where one orientation of something causes a change in the orientation of something larger. Imagine a lot of activity in a flat field with a butterfly, a bird, a cat, a dog, a person, a bike, a car, and a truck, all traveling in different directions. The direction of each is a point in a circle, collectively a point on an eight-dimensional torus $\mathbb{T}^8$.

A butterfly flaps its wings;
a nearby bird changes direction;
a running cat watching the bird swerves;
a dog swerves at the motion of the cat;
a walking person swerves to avoid hitting the dog;
a passing bicycle swerves a bit;
causing a passing car to change its direction;
a truck changes directions in response.

The butterfly flapping its wings cascades to ever larger scales, perhaps to Texas-sized scales containing tornadoes. All of these changes in directions need not affect the energy of each component. Or we can follow Lorenz, who investigates packets of air of different sizes, small packets perturbing larger packets, in increasing sequence of increasingly large air packets. Each packet is twice the diameter of its predecessor [2]. Tiny initial perturbations throughout the small-scale packets grow quickly and together become a large-scale perturbation. In this sense, one butterfly flapping its wings in the smallest packet under consideration totally changes the direction of the largest-scale tornado environment, shifting the tornado perhaps from Oklahoma to Texas, or vice versa. Oklahoma and Texas are adjacent states in the USA. These are among the places in the world with the most severe tornado weather.

The perturbations keep influencing the larger scales, adding ever-increasing perturbations to the direction of the next larger packet. The time scale for the perturbations to occur is shorter for the small scales than for the larger scales, but we ignore this inconsistency.

4. Numerical Investigations

We use a superscript to denote the iterate number of vectors such as ϕ, θ, and ψ and a subscript for coordinate number. Choose initial vectors $\phi, \theta \in \mathbb{T}^K$ so that only the first coordinates (denoted by subscripts) have a difference: $(\phi - \theta)_1 := \phi_1 - \theta_1 = 10^{-30}$, and for coordinate $k > 1$, $(\phi - \theta)_k := \phi_k - \theta_k = 0$. We find that the 20th coordinate of the 300th iterate of M is approximately $\frac{1}{2}$, i.e.,

$$(\phi - \theta)_{20}^{300} = M^{300}(\phi - \theta)_{20} \bmod 1 \approx \frac{1}{2}.$$

Note that the value $\frac{1}{2}$ is the maximum possible difference since ϕ_k and θ_k are in a circle where the maximum distance between two points is $\frac{1}{2}$.

We can think of different θ_ks as representing behaviors at different scales of different swirls in the atmosphere, consecutive scales representing the size differences of a factor of 2. Perhaps we can say that a typical butterfly has a size of roughly 0.06 meters, while tornado weather patterns have a scale of at least 10^6 meters, which is the approximate width of Texas. These differ by roughly 2^{24} (or more precisely 23.99). Each swirl can change the direction of the next higher swirl. In order to realistically scale the butterfly problem is $K \approx 24$ for our skew-product system Equation (14). Each swirl might be twice the scale of the next smaller scale.

Of course, there is an immense number of air packets that are the size of a butterfly, and perturbations in each might affect some next larger packet. An intermediate-size packet might be perturbed by several smaller packets. However, here, we look only at a single cascade starting with one butterfly, and for each packet, we only look at its influence on one larger packet. Realistically, the time of propagation from the kth packet to the larger $(k+1)^{\text{st}}$ is longer as k increases, a fact that our maps do not reflect.

A moving peak of the distribution. In the following Table 1, define

$$C(n) := \binom{n}{n/2}$$

for $n = 2, 4, 6, \ldots$. It is the magnitude of the largest coordinate of $M^n e_1$ where $e_1 = (1, 0, 0, \ldots)$ for the case of unbounded space. Hence the location of the peak value is at $\frac{n}{2}$. This location moves to larger values as time n increases.

The number $C(n)^{1/n}$ is a finite-time geometric growth rate (which approaches 2 as can be seen in the table). This value approaches 2, but it is showing that as n increases, some circle (namely circle # $n/2$) is strongly affected by the initial tiny perturbation. See also Figure 2.

Table 1. **The magnitude of the largest coordinate $\binom{n}{n/2}$ of $M^n e_1$ where $e_1 = (1, 0, 0, \ldots)$.** Convergence of the right column to 2 is slow as n increases.

n	$C(n) = \binom{n}{n/2}$	$C(n)^{1/n}$
2	2	1.414214
4	6	1.565086
22	705,432	1.844331
24	2,704,156	1.853537
26	10,400,600	1.861602
100	1.009×10^{29}	1.950018

Sensitivity is about the behavior of the difference between two different trajectories. Since the equations we study are linear, we can write the equations for such a difference. Let $\psi = \phi - \theta$ where ϕ and θ are two trajectories. Then, the difference ψ satisfies

$$\psi = (\psi_1, \psi_2 \ldots, \psi_K) \mapsto (\psi_1, \psi_2 + \psi_1, \ldots, \psi_K + \psi_{K-1}) \mod 1. \tag{16}$$

This equation without mod 1 is the mosquito model (9). In that case, the sum of coordinates of ψ doubles each iterate in the unbounded case where K is infinite. We consider two trajectories whose initial conditions differ only in the first coordinate. In Figure 3, we see the growth in the difference in coordinate k of ψ between two trajectories with respect to n. It asymptotically converges to an exponential growth.
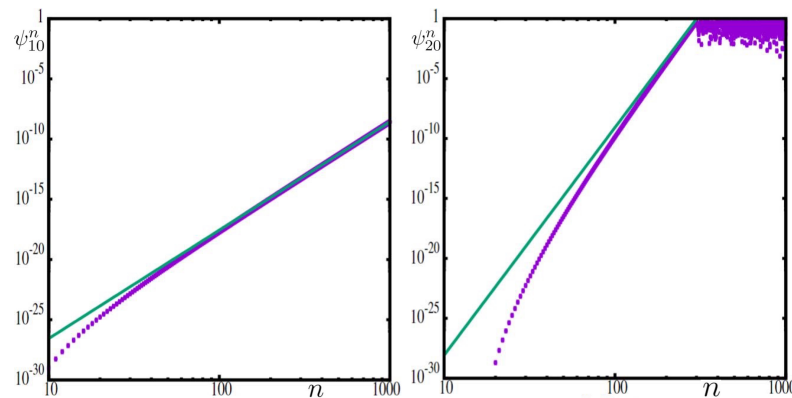
Figure 3. For Equation (16), the growth in a ψ coordinate of the difference between two trajectories. The initial condition for the difference ψ is chosen with the first coordinate $\psi_1 = 10^{-30}$, and all other coordinates are 0. Notice that, for each k, $\psi_k^n=0$ for iterate n when $n < k$. (**Left**), $\boldsymbol{\psi_{10}^n}$. The dots plot ψ_{10}^n as a function of the number of iterates n of the map, and the straight line (green) is $C_1 \cdot n^9$, where C_1 is chosen so that the line and the curve are tangent. (**Right**), $\boldsymbol{\psi_{20}^n}$. This panel is similar to the left panel using the straight line $C_2 \cdot n^{19}$. The green lines have "slopes" $s = 9$ and 19 in our "log log" plot, respectively, i.e., $\log(\psi_{10}^n \text{ or } \psi_{20}^n) = s \cdot \log(n) + \text{constant}$. This fact does not depend on the base of the logs since the slope is the ratio of two logs with the same base.

5. Occasional Closest Approach of Two Trajectories

In this section, we discuss the mathematical aspects of the map F in Equation (14) concerning the degree of complexity.

Scrambled pairs. For a map F, we say a pair ϕ, θ of points in the space is **scrambled** [20] if

$$\liminf_{n \to \infty} \text{dist}(F^n(\phi), F^n(\theta)) = 0 \quad \text{and} \quad \limsup_{n \to \infty} \text{dist}(F^n(\phi), F^n(\theta)) > 0.$$

For the map Equation (14), the first coordinate of $F^n(\phi) - F^n(\theta)$ is independent of n. Hence, the infimum of the distance between $F^n(\phi)$ and $F^n(\theta)$ could go to zero only if we choose two points with the same first coordinate.

Let $\mathcal{P}$ be a set of pairs of points. Let **diam($\mathcal{P}$)** denote the maximum possible distance between pairs in $\mathcal{P}$. We say a pair ϕ, θ in $\mathcal{P}$ is **totally scrambled** (in $\mathcal{P}$) if the pair is scrambled and satisfies

$$\limsup_{n \to \infty} \text{dist}(F^n(\phi), F^n(\theta)) = \text{diam}(\mathcal{P}).$$

Conjecture 1. *For the map Equation (14) on $\mathbb{T}^K$ for $K > 2$, let $\mathcal{P}$ be the set of pairs ϕ, θ whose first coordinates are equal. Then, almost every pair ϕ, θ in $\mathcal{P}$ is totally scrambled.*

We describe the numerical evidence for this conjecture later in this section. Notice that $\mathcal{P}$ is invariant: for each pair ϕ, θ in $\mathcal{P}$, the pair $(F^n(\phi), F^n(\theta))$ is in $\mathcal{P}$ for all $n > 0$.

Results for the map Equation (14) when α is irrational. The following theorems by Furstenberg [19] are fundamental results for the map (14). See also Furstenberg Theorem 4.21 (p. 116) and Corollary 4.22 of the book [18].

Theorem 1. *The map is minimal (every orbit is dense).*

Recall: A Borel set is any set that can be formed from open sets through the operations of countable union, countable intersection, and complements.

Theorem 2. *The map is uniquely ergodic (there is only one invariant Borel probability measure).*

Since the map Equation (14) preserves the Lebesgue measure, its unique ergodicity implies its minimality. In general, minimality does not imply unique ergodicity, for example, interval exchange transformations (IET).

Numerical evidence for our conjecture. Two trajectories might occasionally move close together, only to diverge, repeating this pattern in a non-periodic or apparently stochastic manner. In Figure 4, we can see that the closest approach $y(N)$ between two trajectories during the time interval $[0, N]$ decreases as time N increases and converges to 0. It supports the first condition of the above conjecture. The decay rate of the closest difference at time N seems to obey a power law which can be explained below. Suppose we choose N random points using a uniform distribution on a D-dimensional box $[0, \frac{1}{2}]^D$. For $0 < \varepsilon < \frac{1}{2}$, when choosing N random independent points, the expected number of points in $[0, \varepsilon]^D$ is $(2\varepsilon)^D N$. If we choose ε so that the expected number is 1, we obtain $(2\varepsilon)^D = N^{-1}$, i.e., $2\varepsilon = N^{\frac{-1}{D}}$. In our case, $D = K - 1$. Thus, we plot $\varepsilon = \frac{1}{2} N^{\frac{-1}{K-1}}$ on a log-log scale which yields a straight line $\frac{-1}{K-1} \log(N) - \log 2$ with slope $-\frac{1}{K-1}$. For such an ε, given N, the probability that none of the N points are in the $[0, \varepsilon]^D$ is $(1 - (\frac{2}{\varepsilon})^D)^N = (1 - \frac{1}{N})^N \approx \frac{1}{e}$. Figure 4 shows that the difference between two trajectories behaves in this manner. Note that, if two values of N are chosen close together, whether the plotted points on curves are above or below the line is correlated.
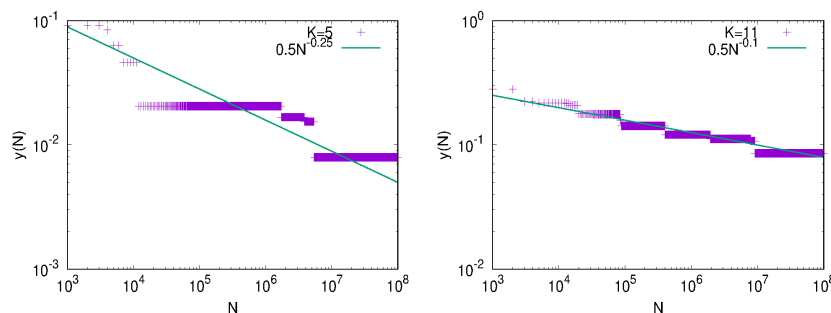

Figure 4. Closest approach between two trajectories θ^n and ϕ^n up to time N. The initial points θ_1^0, ϕ_1^0 were chosen at random. For coordinates $k = 2, \cdots, K$, at time n, define $\delta^n := \max_{k=2,\cdots,K} |\theta_k^n - \phi_k^n|$. Notice coordinate $k = 1$ is excluded since for all $n > 0$, $\theta_1^n - \phi_1^n = \theta_1^0 - \phi_1^0$ is constant. The **(left)** panel is for dimension $K = 5$ and the **(right)** is for $K = 11$. For both, we plot $y(N) := \min_{n \leq N} \delta^n$, the closest approach between two trajectories θ and ϕ on $[1, N]$. This is non-increasing as N increases. For comparison, we also plot $y = \frac{1}{2} N^{-\frac{1}{K-1}}$, which in this log-log plot is a straight line with slope $\frac{-1}{K-1}$.

6. Discussion

6.1. Summary

We present linear models exhibiting large-scale rapid growth that is not reflected in the Lyapunov exponent of the model since there exist no positive Lyapunov exponents. The growth of solutions is due to off-diagonal terms. The off-diagonal terms correspond, in our case, to spatial transmission. This is an often-discussed topic, but our treatment is different in that, here, our system is linear. Since M is a lower-triangular matrix, the off-diagonal terms do not affect the eigenvalue(s) of M. We observe an initial exponential growth in the total number of infected mosquitoes, but the exponential growth is only transient. Note that this is not a chaotic transient [21], as there is no chaotic invariant set.

These models present an alternative source for the sensitivity to initial conditions present in complex systems. See Sander and Yorke [22] for a discussion of some of the many definitions of chaos that reflect different aspects of chaos.

6.2. Zika-Infected Mosquitoes in Miami, Florida, USA

The problem of containing and controlling Zika-infected mosquitoes is based on an actual outbreak in the Americas and specifically in Miami, Florida, where it was a localized

outbreak. The New York Times published articles about Zika in Miami with the titles. (The online titles may differ from the print version's titles).

- (3 February 2016) "Fighting the Zika Virus. Subtitle: The World Health Organization was right to declare the mosquito-borne disease an international public health emergency" (by the Editorial Board)
- (1 April 2016) "In Miami, Facing Risk of Zika With Resolve but Limited Resources. Subtitle: Stopping the virus's spread, health experts say, requires vigorous control of the mosquitoes that carry it."
- (9 August 2016) "Zika Cases Rise in Miami, and Officials Try to Soothe Fears"
- (print edition 10 August 2016, page A3) "Zika Cases Rise in Miami, but Remain Contained"

Our simplified model shows that a local outbreak can be treated locally with insecticides, but there is a risk of a rapidly growing outbreak. In particular, it is not necessary to treat all of Miami with insecticides. We rejected the alternative approach of treating the problem of mosquitoes with partial differential equations with diffusion, thereby creating a model no politician in Miami could understand.

6.3. Related Works

Other than simple temporal chaos, complexity in dynamical systems can be generated by several mechanisms, some of which are similar to those in our simple map in some sense. See [21].

Works on Kaneko and Crutchfield on coupled map lattices. There is of course, a huge literature on pipe flow where there can be a moving localized region of turbulence, outside of which the flow is laminar. This can be seen in the earlier paper by Briggs [23] for a similar phenomenon called convective instability in plasma physics. Kerswell [24] is a more recent discussion of pipe flow with real fluid turbulence.

In Kaneko's study [25] of a coupled map lattice model of pipe flow, the isolated regions of chaos move at a fixed rate. To detect the chaos, he uses a moving frame of reference to compute the co-moving Lyapunov exponent, which is related to the propagation of the disturbance in space.

There is also a study [15] on the following coupled system of the Nagumo map, each of which has stably periodic dynamics, but the total system shows similar behavior to that shown in spatio-temporal chaotic dynamics:

$$x_k^{n+1} = \frac{1}{2r+1} \sum_{j=-r}^{r} f(x_{k+j}^n), \tag{17}$$

where $f(x) = sx + \omega \pmod 1$ for some real values s and ω, and $x_k^n \in [0,1)$ is the state at the kth site ($k = 0, \dots, K-1$) at time n, r the radius of the coupling, and K the number of sites. In their work, r is fixed as 1, meaning the nearest neighbor coupling. Even if the local dynamics is periodic under conditions such as $s = 0.91, \omega = 0.1$, when it is coupled into a spatial system, "turbulent" behavior can exist for times that grow faster than exponentially with increasing system volume.

Spatially varying chaos. Nonlocally coupled oscillators can exhibit complex spatio-temporal patterns called chimera states, consisting of coexisting domains of spatially coherent (synchronized) and incoherent dynamics [26]. High-dimensional coupled Kuramoto oscillators can show chaotic behavior, although a single oscillator behaves periodically without mutual interactions [27–29]. It is also well known that the degree of chaos in the Kuramoto–Sivashinsky system becomes higher as the spatial size increases [30,31]. The system can show so-called spatio-temporal chaos.

Strange nonchaotic attractor (SNA) [32–34]. The skew-product map above and SNA models have an irrational rotation as in Equation (12). Both can show rapid growth, but neither has a positive Lyapunov exponent. SNA models are nonlinear and usually two-dimensional, whereas our maps are linear and high-dimensional.

References

1. Lorenz, E.N. Deterministic nonperiodic flow. *J. Atmos. Sci.* **1963**, *20*, 130–141. [CrossRef]
2. Lorenz, E.N. The predictability of a flow which possesses many scales of motion. *Tellus* **1969**, *21*, 289–307. [CrossRef]
3. Banks, J.; Brooks, J.; Cairns, G.; Davis, G.; Stacey, P. On Devaney's definition of chaos. *Am. Math. Mon.* **1992**, *99*, 332–334. [CrossRef]
4. Glasner, E.; Weiss, B. Sensitive dependence on initial conditions. *Nonlinearity* **1993**, *6*, 1067. [CrossRef]
5. Guckenheimer, J. Sensitive dependence to initial conditions for one dimensional maps. *Commun. Math. Phys.* **1979**, *70*, 133–160. [CrossRef]
6. Ruelle, D. Small random perturbations of dynamical systems and the definition of attractors. *Commun. Math. Phys.* **1981**, *82*, 137–151. [CrossRef]
7. Franklin, B. *Poor Richard's Almanack*; Barnes & Noble Publishing: New York, NY, USA, 2004.
8. Lorenz, E.N. The butterfly effect. In *Premio Felice Pietro Chisesi e Caterina. Tomassoni award Lecture*; University of Rome: Rome, Italy, 2008.
9. Shen, B.W.; Pielke, R.A.; Zeng, X.; Cui, J.; Faghih-Naini, S.; Paxson, W.; Atlas, R. Three Kinds of Butterfly Effects within Lorenz Models. *Encyclopedia* **2022**, *2*, 1250–1259. [CrossRef]
10. Wikipedia. Butterfly Effect—Wikipedia, The Free Encyclopedia. Available online: http://en.wikipedia.org/w/index.php?title=Butterfly%20effect&oldid=1140833034 (accessed on 24 March 2023).
11. Shen, B.W.; Pielke, R.A.; Zeng, X. One Saddle Point and Two Types of Sensitivities within the Lorenz 1963 and 1969 Models. *Atmosphere* **2022**, *13*, 753. [CrossRef]
12. Demers, J.; Bewick, S.; Agusto, F.; Caillouët, K.A.; Fagan, W.F.; Robertson, S.L. Managing disease outbreaks: The importance of vector mobility and spatially heterogeneous control. *PLoS Comput. Biol.* **2020**, *16*, e1008136. [CrossRef]
13. Yamada, M.; Ohkitani, K. Lyapunov spectrum of a chaotic model of three-dimensional turbulence. *J. Phys. Soc. Jpn.* **1987**, *56*, 4210–4213. [CrossRef]
14. Kulkarni, D.; Schmidt, D.; Tsui, S.K. Eigenvalues of tridiagonal pseudo-Toeplitz matrices. *Linear Algebra Its Appl.* **1999**, *297*, 63–80. [CrossRef]
15. Crutchfield, J.P.; Kaneko, K. Are attractors relevant to turbulence? *Phys. Rev. Lett.* **1988**, *60*, 2715. [CrossRef]
16. Assani, I. Wiener-Wintner Ergodic Theorem, in Brief. *Not. Am. Math. Soc.* **2022**, *69*, 198–209. [CrossRef]
17. Auslander, J. *Minimal Flows and Their Extensions*; Elsevier: Amsterdam, The Netherlands, 1988.
18. Einsiedler, M.; Ward, T. *Ergodic Theory*; Springer: Berlin/Heidelberg, Germany, 2013; Volume 4, pp. 4–5.
19. Furstenberg, H. Strict ergodicity and transformation of the torus. *Am. J. Math.* **1961**, *83*, 573–601. [CrossRef]
20. Li, T.Y.; Yorke, J.A. Period Three Implies Chaos. *Am. Math. Mon.* **1975**, *82*, 985–992. [CrossRef]
21. Lai, Y.C.; Tél, T. *Transient Chaos: Complex Dynamics on Finite Time Scales*; Springer: New York, NY, USA, 2011; Volume 173.
22. Sander, E.; Yorke, J.A. The Many Facets of Chaos. *Int. J. Bifurc. Chaos* **2015**, *25*, 1530011. [CrossRef]
23. Briggs, R.J. *Electron-Stream Interaction with Plasmas*; MIT Press: Cambridge, MA, USA, 1964.
24. Kerswell, R.R. Recent progress in understanding the transition to turbulence in a pipe. *Nonlinearity* **2005**, *18*, R17. [CrossRef]
25. Kaneko, K. Lyapunov analysis and information flow in coupled map lattices. *Phys. D Nonlinear Phenom.* **1986**, *23*, 436–447. [CrossRef]
26. Omelchenko, I.; Omel'chenko, E.; Hövel, P.; Schöll, E. When nonlocal coupling between oscillators becomes stronger: Patched synchrony or multichimera states. *Phys. Rev. Lett.* **2013**, *110*, 224101. [CrossRef]
27. Girnyk, T.; Hasler, M.; Maistrenko, Y. Multistability of twisted states in non-locally coupled Kuramoto-type models. *Chaos Interdiscip. J. Nonlinear Sci.* **2012**, *22*, 013114. [CrossRef]
28. Jensen, M.H.; Bak, P. Spatial chaos. *Phys. Scr.* **1985**, *1985*, 64. [CrossRef]
29. Omelchenko, I.; Maistrenko, Y.; Hövel, P.; Schöll, E. Loss of coherence in dynamical networks: Spatial chaos and chimera states. *Phys. Rev. Lett.* **2011**, *106*, 234102. [CrossRef] [PubMed]

30. Kuramoto, Y. Diffusion-induced chaos in reaction systems. *Prog. Theor. Phys. Suppl.* **1978**, *64*, 346–367. [CrossRef]
31. Toh, S. Statistical Model with Localized Structures Describing the Spatio-Temporal Chaos of Kuramoto-Sivashinsky Equation. *J. Phys. Soc. Jpn.* **1987**, *56*, 949–962. [CrossRef]
32. Glendinning, P.; Jäger, T.; Keller, G. How chaotic are strange non-chaotic attractors? *Nonlinearity* **2006**, *19*, 2005–2022. [CrossRef]
33. Grebogi, C.; Ott, E.; Pelikan, S.; Yorke, J.A. Strange attractors that are not chaotic. *Phys. Nonlinear Phenom.* **1984**, *13*, 261–268. [CrossRef]
34. Pikovsky, A.S.; Feudel, U.; Kuznetsov, S.P. *Strange Nonchaotic Attractors: Dynamics between Order and Chaos in Quasiperiodically Forced Systems*; World Scientific: Toh Tuck Link, Singapore, 2006; Volume 56.